10.1109/ULTSYM.2010.0468

Rapid Measurement of Ultrasound Transducer Fields in Water Employing Compressive Sensing

Martin Schiffner and Georg Schmitz
Institute of Medical Engineering, Ruhr-University Bochum, D-44801 Bochum, Germany, Email: martin.schiffner@rub.de

***Abstract*—The quantitative measurement of acoustic pressure fields in fluids is of crucial interest for the design of medical ultrasound transducers. A new measurement technique for the radiated ultrasound beams using the concept of compressive sensing is introduced. In this approach, a regular grid is defined on a plane oriented perpendicular to the preferred direction of the sound beam. Waveforms are measured at random positions on this grid and are decomposed into their frequency components. The frequency components of missing waveforms in this grid can then be reconstructed exploiting the compressibility of the associated angular spectra. The feasibility of our concept is demonstrated by experiments in a water reservoir with a spherically focused circular single element transducer. Using two different excitation voltages and only 25 % of the recommended number of measurements in literature, the original sound fields could be reconstructed with relative mean squared errors (MSEs) of 11.4 % and 6.86 %, respectively. The relative MSEs obtained by a standard interpolation method were 12.68 % and 7.05 % in these cases.**

I. Introduction

The quantitative measurement of acoustic pressure fields in fluids is of crucial interest for the design of medical ultrasound transducers and for the development as well as optimization of beamforming concepts in diagnostic ultrasound imaging systems [1]. However, the spatially dense, computer-controlled sampling of volumes by a hydrophone is time-consuming. On the one hand high spatial frequencies may occur within the pressure field demanding high spatial sampling rates. On the other hand averaging procedures used to mitigate the influence of noise slow down measurements.

In this contribution we introduce a new approach to the measurement of acoustic pressure in sound beams employing the concept of compressive sensing (CS) [2], [3]. We define a regular grid on a plane oriented perpendicular to the preferred direction of the sound beam. We acquire waveforms at random positions on this grid. The frequency components contained in these waveforms are used to reconstruct the frequency components of missing waveforms in this grid by exploiting the compressibility of the associated angular spectra [4] and by solving a convex optimization problem.

Our method demonstrates, that the number of measurements required to adequately quantify the acoustic pressure within a sound beam can be reduced to a great extent without distorting the results.

This contribution consists of three sections. First, the mathematical framework of our approach is presented. The angular spectrum of plane waves as well as CS are introduced. Next, results of the experimental validation of our new method are shown. They are compared to results obtained by interpolation based on the discrete Fourier transform (DFT). In the last section the advantages of our strategy will be pointed out.

II. Mathematical Framework

Our approach is based on the assumption, that the angular spectra associated with the complex phasors of the acoustic pressure on planes perpendicular to the preferred direction of a sound beam are compressible. According to [2] this means, that only a few significant frequency components exist. These can be recovered using CS. Both concepts, the angular spectrum as well as CS, will be introduced in the following.

A. The Angular Spectrum of Plane Waves

According to [1], [4], the complex phasor associated with a monofrequent acoustic pressure field can be Fourier transformed across any plane in spatial domain. The frequency components of the resulting two-dimensional spectrum represent a decomposition of the pressure field on this plane into plane progressive sound waves. Each spatial frequency is related to a plane sound wave traveling in a distinct direction away from that plane.

Let $\mathbf{e}_x$, $\mathbf{e}_y$ and $\mathbf{e}_z$ denote the unit vectors in the directions of the positive coordinate axes in a Cartesian coordinate system. Further, let $\mathbf{r} \in \mathbb{R}^3$ with $\mathbf{r} = x\mathbf{e}_x + y\mathbf{e}_y + z\mathbf{e}_z$ be a spatial coordinate and let $p : \mathbb{R}^3 \mapsto \mathbb{C}$ denote the complex phasor associated with the monofrequent acoustic pressure $\tilde{p}$ in time domain. The latter are related via the identity

$$\tilde{p}(\mathbf{r}, t) = \mathrm{Re}\left\{p(\mathbf{r})e^{j\omega t}\right\},$$

where Re extracts the real part, $\omega = 2\pi f$ indicates the angular frequency derived from frequency f, and t is continuous time. In linear acoustics, the complex phasor p is governed by the well-known Helmholtz equation

$$\Delta p(\mathbf{r}) + k^2(\mathbf{r}) = 0 \tag{1}$$

for all source-free points, where Δ denotes the Laplace operator and $k = 2\pi/\lambda$ is the frequency-dependent wave number with λ as wave length. Its solution set for the free space partly consists of plane progressive waves. Let $\mathbf{k} = k_x\mathbf{e}_x + k_y\mathbf{e}_y + k_z\mathbf{e}_z$ indicate the wave vector with l_2-norm (Euclidean length)

$$\|\mathbf{k}\|_2 = \sqrt{k_x^2 + k_y^2 + k_z^2} = k. \tag{2}$$

A plane progressive sound wave with complex amplitude $A(\mathbf{k})$ traveling in the direction of $-\mathbf{k}$ and satisfying (1) is then given by

$$p_{\mathbf{k}}(\mathbf{r}) = A(\mathbf{k})e^{j\langle \mathbf{k},\mathbf{r}\rangle}. \tag{3}$$

The phasor p on a plane with constant z-coordinate can be expressed by the two-dimensional inverse Fourier transform

$$p(\mathbf{r}) = \frac{1}{(2\pi)^2}\int_{\mathbb{R}^2} P(k_x,k_y,z)e^{j(k_x x+k_y y)}d(k_x,k_y). \tag{4}$$

The spatial spectrum P is called angular spectrum. A sound beam generated by a medical ultrasound transducer can usually be regarded as a superposition of plane waves with a preferred direction of propagation away from the transducer. Without loss of generality we assume that this direction is $\mathbf{e}_z$. Due to (2), the wave vectors of the plane waves then satisfy $|k_x|, |k_y| \ll |k_z| \leq k$. Plane waves whose wave vectors violate this condition ideally do not exist and $A(\mathbf{k}) = 0$. If $k_z < 0$, the angular spectrum is uniquely related to the complex amplitudes of the plane waves (3) by

$$A\big[\mathbf{g}(k_x,k_y)\big] = \frac{\sqrt{k^2-k_x^2-k_y^2}e^{j\sqrt{k^2-k_x^2-k_y^2}z}}{(2\pi)^2 k}P(k_x,k_y,z) \tag{5}$$

with

$$\mathbf{g}(k_x,k_y) = k_x\mathbf{e}_x + k_y\mathbf{e}_y - \sqrt{k^2-k_x^2-k_y^2}\,\mathbf{e}_z \tag{6}$$

for $k_x^2+k_y^2 < k^2$. Consequently, the angular spectrum of a sound beam exhibits low-pass characteristics.

In a real sound beam, also spectral components which satisfy $k_x^2+k_y^2 > k^2$ might arise. These are associated with evanescent waves which are unable to propagate according to (1). Following [4], these components are attenuated exponentially and do not carry energy.

B. Compressive Sensing

Consider the complex phasor p on a plane with constant z-coordinate. Sampling along the x- and y-axes in intervals of lengths Δx and Δy , respectively, yields

$$p[n_x,n_y] = p(n_x\Delta x, n_y\Delta y, z) \tag{7}$$

for $0 \leq n_x \leq N_x-1$ and $0 \leq n_y \leq N_y-1$. The total number of samples is $N = N_xN_y$.

The two-dimensional Fourier basis functions for the samples of p are then given by

$$\psi_{l_x,l_y}[n_x,n_y] = \frac{1}{\sqrt{N}}e^{j\left(K_{x,l_x}n_x+K_{y,l_y}n_y\right)} \tag{8}$$

where $K_{x,l_x} = 2\pi l_x/N_x$ and $K_{y,l_y} = 2\pi l_y/N_y$ denote the normalized angular spatial frequencies in x- and y-direction, respectively. The indices can be adjusted in the intervals $0 \leq l_x \leq N_x-1$ and $0 \leq l_y \leq N_y-1$. The phasors (7) can be represented in terms of their discrete angular spectrum P by using (8). Thus, the identity

$$p[n_x,n_y] = \sum_{l_x=0}^{N_x-1}\sum_{l_y=0}^{N_y-1} P[l_x,l_y]\psi_{l_x,l_y}[n_x,n_y] \tag{9}$$

holds. Employing vector-matrix notation, we define the complex-valued $N \times 1$ vectors

$$\begin{aligned}\mathbf{p} = \big(&p[0,0],\ldots,p[0,N_y-1],p[1,0],\ldots,p[1,N_y-1],\\ &\ldots p[N_x-1,0],\ldots,p[N_x-1,N_y-1]\big)^{\mathrm{T}},\end{aligned} \tag{10}$$

$$\begin{aligned}\mathbf{P} = \big(&P[0,0],\ldots,P[0,N_y-1],P[1,0],\ldots,P[1,N_y-1],\\ &\ldots,P[N_x-1,0],\ldots,P[N_x-1,N_y-1]\big)^{\mathrm{T}},\end{aligned} \tag{11}$$

$$\begin{aligned}\boldsymbol{\psi}_{l_x,l_y} = \big(&\psi_{l_x,l_y}[0,0],\ldots,\psi_{l_x,l_y}[0,N_y-1],\\ &\psi_{l_x,l_y}[1,0],\ldots,\psi_{l_x,l_y}[1,N_y-1],\ldots,\\ &\psi_{l_x,l_y}[N_x-1,0],\ldots,\psi_{l_x,l_y}[N_x-1,N_y-1]\big)^{\mathrm{T}},\end{aligned} \tag{12}$$

and the $N \times N$ matrix

$$\begin{aligned}\boldsymbol{\Psi} = \big(&\boldsymbol{\psi}_{0,0},\ldots,\boldsymbol{\psi}_{0,N_y-1},\boldsymbol{\psi}_{1,0},\ldots,\boldsymbol{\psi}_{1,N_y-1},\\ &\ldots,\boldsymbol{\psi}_{N_x-1,0},\ldots,\boldsymbol{\psi}_{N_x-1,N_y-1}\big).\end{aligned} \tag{13}$$

The linear combination (9) can now be expressed by

$$\mathbf{p} = \boldsymbol{\Psi}\mathbf{P}. \tag{14}$$

In Section II-A, the angular spectrum (4) of the complex phasors in a sound beam with the preferred direction $\mathbf{e}_z$ was investigated. It was shown to exhibit low-pass characteristics provided the Fourier transform is carried out on a plane with constant z-coordinate. Assuming sufficiently small spatial sampling intervals Δx and Δy, the discrete angular spectrum (11) is compressible. According to [2], [3], $\mathbf{P}$ can then be recovered with small relative mean squared error (MSE) from $M \ll N$ random linear projections of $\mathbf{p}$ described by

$$\mathbf{y} = \boldsymbol{\Xi}\mathbf{p} = \boldsymbol{\Xi}\boldsymbol{\Psi}\mathbf{P}. \tag{15}$$

In order to recover $\mathbf{P}$ from $\mathbf{y}$, the convex optimization problem

$$\hat{\mathbf{P}} = \underset{\mathbf{x}\in\mathbb{C}^N}{\arg\min}\{\|\mathbf{x}\|_1\} \text{ subject to } \mathbf{y} = \boldsymbol{\Xi}\boldsymbol{\Psi}\mathbf{x} \tag{16}$$

has to be solved. The recovered phasors are given by the inverse two-dimensional DFT $\hat{\mathbf{p}} = \boldsymbol{\Psi}\hat{\mathbf{P}}$.

In our approach the $M \times N$ matrix $\boldsymbol{\Xi}$ contained exactly one unity entry in each row. The column of the unity entry was chosen randomly employing a discrete uniform distribution. All rows of $\boldsymbol{\Xi}$ were different. This choice corresponds to M unique measurements of (7) at random positions. Following [5], our measurement matrix $\boldsymbol{\Xi}\boldsymbol{\Psi}$ satisfies the restricted isometry property (RIP) with high probability, if M is large enough. This means that (16) recovers sparse angular spectra exactly. The optimization problem was solved efficiently using the algorithm SPGL1 [6].

III. Experimental Validation

A. Experimental Setup

The experimental setup is depicted schematically in Fig. 1. An arbitrary function generator (AFG) whose output voltage was amplified by 55 dB excited a spherically focused circular

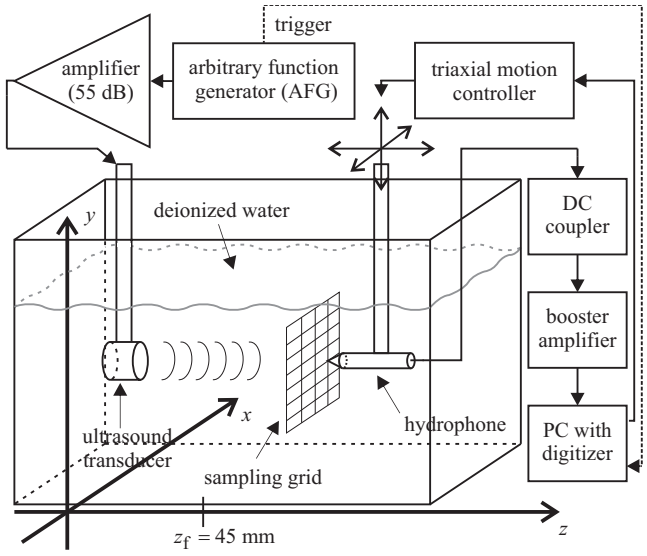

Fig. 1. Schematic drawing of the experimental setup employed to measure the ultrasound beam generated by a spherically focused circular single element transducer.

single element ultrasound transducer (diameter: 12.7 mm, center frequency: $f_c = 2.25$ MHz, focal length: $z_f = 45$ mm). The transducer was submerged in deionized water and its surface was located on the plane $z = 0$. A fully calibrated hydrophone measurement system consisting of a hydrophone (tip diameter: 40 µm), a DC coupler and a booster amplifier converted the resulting acoustic pressure into a voltage. The hydrophone was attached to a triaxial motion system controlled by a standard personal computer. The voltage signal was fed into a digitizer card (sampling rate: 50 MHz, resolution: 12 bit, full scale: 2 V) mounted in this PC.

In our experiments the excitation voltages generated by the AFG were two-cycle sine waves (frequency: f_c, pulse repetition frequency: 40 Hz). Their peak-to-peak amplitudes were $V_{pp,1} = 60$ mV in the first experiment and $V_{pp,2} = 120$ mV in the second experiment. Each excitation of the transducer triggered an acquisition of the resulting pressure waveform. A square-shaped region (side length: 15.9 mm) around the focus in the focal plane $z = z_f$ was regularly sampled by the hydrophone. The lateral sampling distances were $\Delta x = \Delta y = 110$ µm in the direction of the x- and y-axis, respectively. These were derived in accordance with [7] from the transducer's center frequency by assuming a fractional bandwidth of unity. At each measurement position the arithmetic mean of 20 waveforms was stored. This sampling strategy resulted in $N = N_x N_y = 145 \times 145 = 21025$ stored waveforms for the regular grid. All waveforms were low-pass filtered (cutoff frequency: 10 MHz) to attenuate measurement noise and cropped to a length of $N_t = 301$ samples.

The complex phasors associated with the discrete-time waveforms were obtained by DFTs. Since all measured waveforms were real-valued, the knowledge of their phasors for the first $N_\omega = \lceil N_t/2 \rceil = 151$ frequencies was sufficient for their exact representation. Consequently, the measured ultrasound beam on the plane $z = z_f$ could be described by N_ω vectors (10) in both experiments.

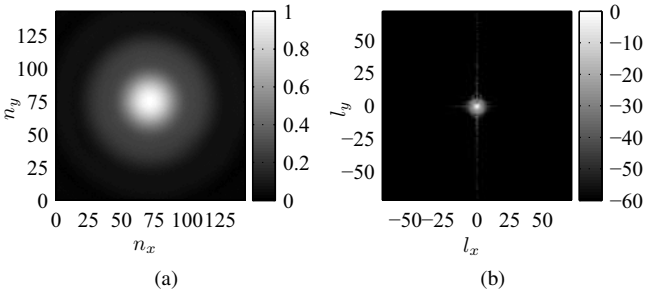

Fig. 2. Normalized magnitudes of the complex phasors (7) for $V_{pp,1} = 60$ mV at a frequency $f \approx 2.16$ MHz near f_c (a) and the associated angular spectrum (9) in dB (b).

In each experiment, our goal was to reconstruct these vectors from $M \ll N$ measured waveforms at random positions by using our CS approach. We simulated the measurement of $M = 5329 \approx N/4$ randomly selected waveforms by generating a measurement matrix $\boldsymbol{\Xi}$ and by evaluating (15) for the N_ω vectors associated with the originally measured waveforms. The phasors (10) were recovered for each frequency by solving (16) and by exploiting $\hat{\mathbf{p}} = \boldsymbol{\Psi}\hat{\mathbf{P}}$. The quality of reconstruction was assessed for each of the N_ω frequencies in terms of the relative MSE defined as

$$\varepsilon_{rel} = \|\mathbf{p} - \hat{\mathbf{p}}\|_2 \,/\, \|\mathbf{p}\|_2 \,. \tag{17}$$

Since the performance of CS depends on the randomly chosen matrix $\boldsymbol{\Xi}$, we repeated the reconstruction 25 times with different versions of $\boldsymbol{\Xi}$.

To evaluate the performance of our method in comparison to regular sampling, the measurement of M waveforms on a regular grid was simulated by neglecting every other waveform in the reference data. The missing phasors for each frequency were recovered using a two-dimensional DFT interpolation. Again, the quality of reconstruction was assessed in terms of the relative MSE (17).

B. Experimental Results

As an example, the magnitudes of the complex phasors (7) for $V_{pp,1}$ at a frequency $f \approx 2.16$ MHz near f_c are illustrated in Fig. 2a. They were normalized by the maximum pressure of $p_{ref} = \max\{p[n_x, n_y]\} \approx 557.9$ kPa. The magnitude in dB of the associated discrete angular spectrum (9) is depicted in Fig. 2b. As predicted in Section II-A, the angular spectrum exhibits strong low-pass characteristics and is clearly compressible.

In a first processing step, the phasors for all N_ω frequencies were reconstructed. The resulting relative MSEs (17) using CS (black, solid) and DFT-based interpolation (light gray, dashed) are depicted in Fig. 3 for $V_{pp,1}$ (a) and $V_{pp,2}$ (b). Moreover, Fig. 3 shows the relative energy distribution of the complex phasors over frequency (dark gray, solid)

$$E_{rel}(f) = \|\mathbf{p}\|_2^2 \,/ \max_f\{\|\mathbf{p}\|_2^2\}. \tag{18}$$

Obviously, both approaches perform well for frequencies around the fundamental frequency f_c as well as for frequencies

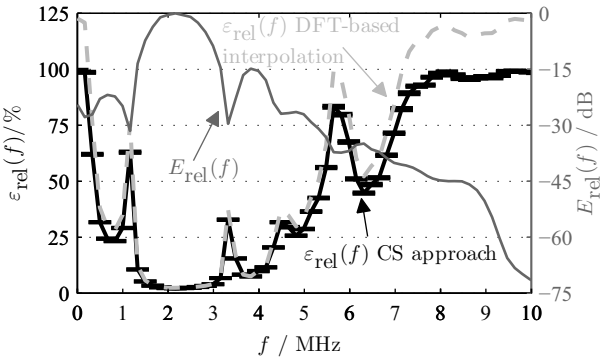

(a) $V_{\mathrm{pp},1} = 60$ mV

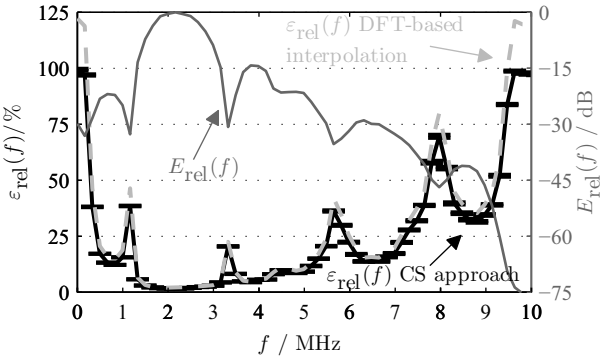

(b) $V_{\mathrm{pp},2} = 120$ mV

Fig. 3. Relative mean squared reconstruction errors (17) and relative energies (18) for $V_{\mathrm{pp},1}$ (a) and $V_{\mathrm{pp},2}$ (b).

near the second harmonic. Around the fundamental frequency a high relative energy (18) can be observed and the relative MSE of CS is about 0.2 % smaller than the relative MSE of DFT-based interpolation. However, as the relative energy decays, our method outperforms DFT-based interpolation in terms of relative MSE by several percent. This can be observed e. g. between 4.5 MHz and 7 MHz for $V_{\mathrm{pp},1}$ as well as between 6 MHz and 9 MHz for $V_{\mathrm{pp},2}$. For frequencies greater than 9 MHz no significant acoustic pressures exist, such that both approaches fail in reconstructing measurement noise. The estimated standard deviations of the relative MSEs obtained by the 25 different matrices $\boldsymbol{\Xi}$ are illustrated by errorbars on the CS curves. The exact choice of $\boldsymbol{\Xi}$ can be considered irrelevant for reconstruction performance.

In a second processing step we investigated the waveforms of acoustic pressure in time domain. For each coordinate $\mathbf{r} = n_x \Delta x \mathbf{e}_x + n_y \Delta y \mathbf{e}_y + z_{\mathrm{f}} \mathbf{e}_z$ on the plane $z = z_{\mathrm{f}}$ the relative MSEs of the reconstructed waveforms were computed. The results are illustrated in Fig. 4 for CS (Fig. 4a and 4c). and for DFT-based interpolation (Fig. 4b and 4d). The mean relative MSEs for all locations were 11.4 % ($V_{\mathrm{pp},1}$) and 6.86 % ($V_{\mathrm{pp},2}$) for our approach as well as 12.68 % ($V_{\mathrm{pp},1}$) and 7.05 % ($V_{\mathrm{pp},2}$) for DFT-based interpolation.

IV. Conclusion

We demonstrated that our new approach to the measurement of acoustic pressure in sound beams using the concept of

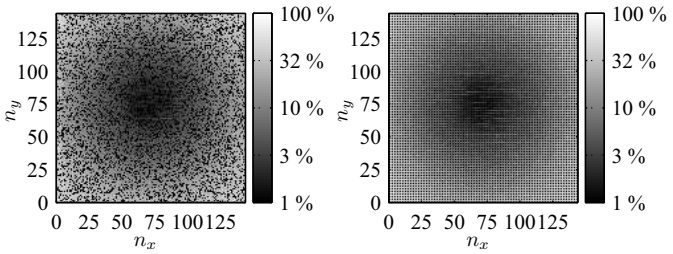

(a) $V_{\mathrm{pp},1} = 60$ mV, CS (b) $V_{\mathrm{pp},1} = 60$ mV, DFT

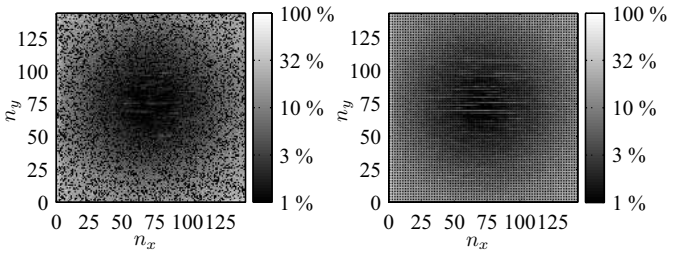

(c) $V_{\mathrm{pp},2} = 120$ mV, CS (d) $V_{\mathrm{pp},2} = 120$ mV, DFT

Fig. 4. Relative mean squared reconstruction errors in time domain for CS and (a), (c) and DFT-based interpolation (b), (d).

compressive sensing is feasible. With only 25 % of the proposed number of measurements (conf. [7]), our method achieves small relative mean squared reconstruction errors. Our new technique outperforms DFT-based interpolation in terms of accuracy and versatility. An arbitrary number of waveforms M can be acquired and used for reconstruction. The measurement of waveforms on a regular grid is no longer necessary. Results indicate that our approach is more robust against measurement noise. The latter causes aliasing artifacts in DFT-based interpolation which decrease reconstruction performance for data with low signal-to-noise ratio. We expect our approach to yield much better results than DFT-based interpolation in sound beams which exhibit more complicated angular spectra, e. g. spectra which are compressible but which do not have low-pass characteristics. These may arise in sound beams emitted by transducer arrays.

References

[1] E. Schafer and P. Lewin, "Transducer characterization using the angular spectrum method," *Journal of the Acoustical Society of America*, vol. 85, no. 5, pp. 2202–2214, May 1989.

[2] R. G. Baraniuk, "Compressive Sensing [Lecture Notes]," *IEEE Signal Processing Magazine*, vol. 24, no. 4, pp. 118–121, July 2007.

[3] D. L. Donoho, "Compressed Sensing," *IEEE Transactions on Information Theory*, vol. 52, no. 4, pp. 1289–1306, April 2006.

[4] J. W. Goodman, *Introduction to Fourier Optics*, 3rd ed. Roberts and Company Publishers, 2004.

[5] M. Rudelson and R. Vershynin, "On Sparse Reconstruction from Fourier and Gaussian Measurements," *Communications on Pure and Applied Mathematics*, vol. 61, no. 8, pp. 1025–1045, August 2008.

[6] E. van den Berg and M. P. Friedlander, "Probing the pareto frontier for basis pursuit solutions," *Journal of Scientific Computing*, vol. 31, no. 2, pp. 890–912, 2008.

[7] R. J. Zemp, J. Tavakkoli, and R. S. C. Cobbold, "Modeling of nonlinear ultrasound propagation in tissue from array transducers," *Journal of the Acoustical Society of America*, vol. 113, no. 1, pp. 139–152, January 2003.